PIK3C2B promotes epithelial to mesenchymal transition and EGFR inhibitors insensitivity in epidermal squamous cell carcinoma.

Silvia Crespo Pomar[1], Anna Borgström[2], Alexandre Arcaro[1] and Roch-Philippe Charles[2*]

[1]University Children's Hospital Bern, Freiburgstrasse 31, 3010 Bern, Switzerland.

[2]Institute of Biochemistry and Molecular Medicine, and Swiss National Center of Competence in Research (NCCR) TransCure, University of Bern, Bühlstrasse 28, 3012 Bern, Switzerland.

Running title: ***PIK3C2B* promotes EMT in epidermal squamous carcinoma cells**

Keywords: *PIK3C2B*, EMT, EGFR, EGFR inhibitor resistance, vesicular traffic

[*]**Corresponding author:** Roch-Philippe Charles, Institute of Biochemistry and Molecular Medicine, University of Bern, Bühlstrasse 28, 3012 Bern, Switzerland.

Phone: +41 31 631 4344 Email: roch-philippe.charles@ibmm.unibe.ch

Disclosure of Potential Conflicts of Interest: The authors have no conflict of interest regarding this publication.

Word count (main body): 3648 **Figure count: 7**

Abstract

While the class I of PI3Ks has been deeply studied due to its clear implication in cancer development, little is known about the class II of PI3Ks. However, recent accumulation of data is now revealing that PI3KC2β, one isoform of this class of PI3Ks, may also play a role in cancer. Specifically, recent studies have suggested an implication of PI3KC2β in metastasis formation through the promotion of epithelial to mesenchymal transition (EMT). Here, we report that the overexpression of PI3KC2β in the epidermal squamous cell carcinoma (ESCC) cells A431 promotes apparent EMT transformation. We further confirm this EMT by showing modification in several biochemical markers (E-cadherin, β-catenin, Snail, Twist1 and Vimentin). Furthermore, an intracellular co-localization of E-cadherin, β-catenin and EGFR was observed. This transformation decreased EGFR signaling and the sensitivity to inhibitors targeting this receptor. To confirm our results, we have used the colon adenocarcinoma cells HT29 and induced overexpression of PI3KC2β in these cells. We could recapitulate in this model some of our major findings regarding EMT in the PI3KC2β overexpressing A431 cells. Taken together, these data support a role of PI3KC2β in promoting EMT.

Introduction

Phosphoinositide-3-kinases (PI3Ks) are a family of lipid kinases that play a role in coordinating main intracellular signaling pathways following the activation by upstream agonists such as receptor tyrosine kinases (RTKs) or G protein coupled receptors (GPCR) (1). They phosphorylate the 3'-hydroxyl group of the inositol ring of three species of phosphatidylinositol (PI) lipid substrates. This triggers the formation of the second messengers PI(3)P (phosphatidylinositol 3-phosphate), PI(3,4)P2 (phosphatidylinositol 3,4-bisphosphate) and PIP3 (phosphatidylinositol 3,4,5-trisphosphate), specifically enriched in different cellular compartments (1). Subsequently, different effectors will be recruited and bind to these PI3K phospholipid products, changing their conformation and inducing the propagation of signals involved in cell cycle progression, cell growth, survival, migration, and intracellular vesicular transport (2).

In mammals, the PI3K family is formed by eight different catalytic PI3K isoforms, classified into three classes (I, II and III), based on sequence homology and *in vitro* substrate specificity (2). The different PI3K isoforms can be expressed in a tissue-specific manner and seem to have non-redundant roles. Among the PI3K classes, mutations in class I PI3K isoforms are especially linked with cancer development, being *PIK3CA* the second most frequently mutated oncogene (3). However, while class I PI3Ks have been well studied, little is known about the function of class II. This is mainly because they were first identified by PCR and homology cloning approaches, not based on their cellular function (4,5). Finally, the lack of specific inhibitors and mouse models hindered the discrimination between the biological functions of each isoform.

PI3KC2β is one of the three isoforms from class II PI3K. It is ubiquitously transcribed, showing the highest levels in placenta and thymus (6,7). This lipid kinase is a monomer mainly activated downstream of RTKs, like EGFR, and other GPCRs (8,9). It has a substrate specificity directed towards PI and PI(4)P, generating a pool of PI(3)P or $PI(3,4)P_2$ in the plasma membrane and endosomes (10,11). Through the recruitment of different secondary messengers and the subsequent activation of AKT/mTOR or RAC signaling pathways, PI3KC2β regulates different cellular functions like cell migration, cell growth, cell survival, invasion, cell cycle progression and K^+ channel activation (12–15).

PI3KC2β is the isoform of the class II of PI3Ks that has the most documented implication in cancer development. Its overexpression at the protein and mRNA level in a variety of human tumors (12,13,16,17), and the promising effects of PI3KC2β inhibition observed in leukemia, brain and neuroendocrine tumors (18), are a few of the observations that support this hypothesis. Recent studies have observed a correlation between PI3KC2β expression and metastasis formation in breast, prostate cancer and esophageal squamous cell carcinoma (12,13,19).

Most of cancer-related death are due to metastases formation. To that end, primary tumors need to undergo the biological process known as epithelial-mesenchymal transition (EMT). This process allows immobile epithelial cells to acquire a mobile mesenchymal phenotype, losing cell-cell contact dependency. This transformation is promoted by the expression of several transcription factors like Snail, Slug, and Twist. Two important mechanisms are the replacement of keratin cytoskeleton by a more plastic Vimentin cytoskeleton and the decreased membranal expression of cell–cell adhesion proteins such as E-cadherin or β-

Catenin (20). Different studies have suggested an implication of PI3KC2β in EMT (12,13). However, the exact mechanism by which this kinase is participating in this process is still unknown.

In the epidermal squamous cell carcinoma (ESCC) cells A431, the overexpression of PI3KC2β has been reported to enhance membrane ruffling, migration speed of the cells, protection from anoikis and cell proliferation (14). We decided to assess if some of these previously reported effects could be consequence of a possible process of EMT induced in these cells after the overexpression of PI3KC2β. For this purpose, A431 cells stably expressing PI3KC2β were evaluated for different EMT markers expression. The cytoplasmic localization of different cell-cell adhesion proteins was also visualized. Moreover, the functional impact of PI3KC2β overexpression was assessed in relation to its effect in EGFR signaling and the sensitivity to inhibitors targeting this receptor. Finally, to further validate our results, PI3KC2β overexpression was induced in an additional cell line, HT29.

Materials and methods

Cell Lines

A431 human epidermoid carcinoma cells and HT29 cells were purchased from the American Type Culture Collection. A431 cells were grown in DMEM (Sigma Aldrich, cat. no. D5796) supplemented with 10% (v/v) fetal bovine serum (FBS) (Gibco, cat. no. 10082147), 2 mM L-glutamine (Gibco, cat. no. 25030081) and 50.000 units of penicillin/streptomycin (Gibco, cat. no. 15140122). HT29 cells were grown in McCoy's 5A Medium (Gibco, cat. no. 26600-023) supplemented with 10% (v/v) fetal bovine serum (FBS) (Gibco, cat. no. 10082147), 2 mM L-

glutamine (Gibco, cat. no. 25030081) and 50.000 units of penicillin/streptomycin (Gibco, cat. no. 15140122). Cells were passaged every 3 to 4 days and were kept incubated in a humidified atmosphere of 5% CO_2 at 37 ˚C. Stably transfected HT29 and A431 clones were grown in the presence of 0.8 mg/ml G418 (Life Technologies).

Stable transfection

A431 cell lines stably expressing PI3KC2β were generated as previously described (8). HT29 cell lines stably expressing PI3KC2β were generated as follows. The cDNA of N-terminal myc-tagged (MEQKLISEEDL) *PI3KC2β* wild-type was cloned into pcDNA3 vector (Invitrogen) using EcoRI and XhoI sites as described in Arcaro et al. 1998. The transfection of the pcDNA3-PI3KC2β plasmid was performed using Lipofectamine 2000 (Invitrogen) according to manufacturer's instructions. 48 h post-transfection cells were split into selection medium containing 1 mg/ml G418. Cells were cultured in the selection medium for 2-3 following weeks. Medium was changed each 72 h. When the single G418 resistant colonies appeared, they were further selected and expanded. After 2-3 passages, expression of PI3KC2β was verified by qPCR and western blot.

Western blotting

Proteins were extracted in RIPA buffer (20 mM Tris-base pH=8, 150 mM NaCl, 1% TritonX-100, 0.1% SDS, 0.5% sodium deoxycholate. Sigma, cat. no. D6750-10G) supplemented with Halt™ protease/phosphatase inhibitor cocktail (Pierce, cat. no. 78444). Protein concentration was assessed by Pierce BCA protein assay kit (Thermo Scientific, cat. no. 23225) and 20 µg of total proteins were

separated by SDS-PAGE. Protein gels were transferred into nitrocellulose membranes and blocked with Tris buffered saline (TBS 1x 130 mM, NaCl 30 mM, Tris-Cl pH=7.5) containing 5% Bovine Serum Albumin (BSA) for 2 h. Western blots were probed with rabbit anti-PI3KC2β polyclonal antibody (1/1000, described in (6), rabbit anti-pAKT S473 (1/1000, Cell signaling, cat. no. 4090), rabbit anti-pERK (1/2000, Cell signaling, cat. no. 4370), mouse anti-panAKT (1/1000, cat. no. 2920, Cell signaling), mouse anti-ERK (1/5000, Cell signaling, cat. no. 9107), mouse anti-β-ACTIN antibody (1/15000, Sigma-Aldrich, cat. no. A5316), mouse anti-E-cadherin (1/1000, Abcam, cat. no. 76055), rabbit anti-β-catenin (1/1000, Abcam, cat. no. 32572) and rabbit anti-EGFR (1/1000, Cell signaling, cat. no. 4267).

Primary antibodies were detected using goat anti-rabbit IR680 (1/10'000, Li-Cor Bioscience, cat. no. 926-68071) and goat anti-mouse IR800 (1/10'000, Li-Cor Bioscience, cat. no. 926-32210) and imaged by a LI-COR OdysseySa® scanner. Antibodies were diluted in TBS x1 containing 2% BSA, 0.1% Tween and 0.1% sodium azide.

Proliferation assays

The EGFR kinase inhibitors, Gefitinib and Erlotinib, were purchased from ChemieTek (Indianapolis, IN, USA). Cells were seeded at a density of 3-5 x 10^3 cells/well (depending on the cell line) in a 96-well plate using the cell line-specific culture medium. Cells were allowed to adhere overnight and were then treated with the indicated concentration of drugs for 72 h. After the treatment, cells were fixed with 10% buffered formalin, stained with 0.2% crystal violet (Sigma-Aldrich, cat. no. C3886-25G) in 2% ethanol, washed 5 times in dH_2O and lysed with 100

µL 1% SDS to recover the dye. Optical density (OD) at 550 nm was measured with a microplate reader and normalized to the DMSO control. Dose-response curves were carried out by using the medium described previously.

Quantitative Real-time PCR

RNA was extracted using the RNeasy Mini Kit (Qiagen, cat. no. 74106) according to the manufacturer's protocol. Reverse-transcription was performed with Superscript II Reverse Transcriptase (Invitrogen, cat. no. 18064-014) following the manufacturer's protocol. The Sybr green® real-time primers used in this project were purchased from Applied Biosystems and are depicted in Table 1. PCR reactions were performed in a ViiA7 cycler (Applied Biosciences) using SybrSelect Mastermix (Applied Biosystems, cat. no. 4472908). Expression of mRNA was normalized to *ACTB* and *GAPDH* housekeeping genes using the $2^{\Delta\Delta ct}$ method.

	qPCR primers	
Gene name	**Forward**	**Reverse**
ACTB	CCT GGC ACC CAG CAC AAT	GGA CAG CGA GGC CAG GAT
EGFR	GCA ATA TCA GCC TTA GGT GCG GCT C	CAT AGA AAG TGA ACA TTT AGG ATG TG
GAPDH	CCA CCC ATG GCA AAT TCC ATG GCA	TCT AGA CGG CAG GTC AGG TCC ACC
PIK3C2B	CAG GCT TCA AGA GGC ACT CA	TGG TCA TCA TTC ACC GTC CG
SNAIL	GGA AGC CCA ACT ATA GCG AGC	CAG TTG AAG ATC TTC CGC GAC
TWIST	CAT CGA CTT CCT CTA CCA GGT C	TCC ATT TTC TCC TTC TCT GGA A

Table 1: list of primers used for qPCR quantifications.

Immunofluorescence staining

Cells were grown for 24 h on glass coverslips in 24 well plates to around 60% confluence. After 10% formalin (Sigma Aldrich, cat. no. HT501128) fixation (10 min), coverslips were washed 3x10 min in phosphate buffered saline (1x PBS: 137 mM NaCl, 2.7 mM KCl, 18 mM KH_2PO_4, 10 mM Na_2HPO_4) and cells were subsequently permeabilized with a 1x PBS, 0.3% TritonX-100 solution. Following blocking with a 1% BSA, 0.2% gelatin, 0.05% saponin in 1x PBS solution and washing with a 0.1% BSA, 0.2% gelatin, 0.05% saponin in 1x PBS solution. Cells were incubated overnight at 4 °C with the primary antibodies, rabbit anti-Vimentin (1/300, Abcam, cat. no. 5741,), mouse anti-E-cadherin (1/200, Abcam, cat. no. 76055), rabbit anti-β-catenin (1/200, Abcam, cat. no. 32572), rabbit anti-EGFR (1/300, Cell Signalling cat. no. 4267), rabbit anti-PI3KC2β polyclonal antibody (1/200, described in (6)), mouse anti-58K (5 µg/ml, cat. Abcam, no. 27043,), mouse anti-RAB 7 (1/300, cat. no. 376362, Santa Cruz Biotechnology) and mouse anti-RAB 11 (1/300, Cell Signalling, cat. no. 5589). The secondary antibodies, goat anti-rabbit Alexa-488 (1:400, Life Technologies, cat. no. A11034) and goat anti-mouse Alexa-633 (1:300, Life Technologies, cat. no. A21052,) were used to detect antigen-antibody complexes; slides were counter-stained with DAPI (500 ng/ml, Sigma Aldrich, cat. no. 32670-25MG) to visualize DNA.

Slide Scanning

Slides were scanned using a Panoramic Midi digital slide scanner (3DHISTECH) and analyzed with the Panoramic Viewer software (3DHISTECH). For the quantification of Vimentin/DAPI positive cells, an area of the slide was selected and analyzed with CellQuant software (3DHISTECH).

208 **Confocal images**

209 Cells were examined by confocal Leica SP8 X STED inverted microscope under 63×
210 magnifications. Image files were collected as a matrix of 1024 × 1024 pixels and
211 analyzed using the Leica Application Suite X Microscope Software.

212

213 **Wound healing assay**

214 Cells were grown to confluency in 6-well tissue culture plates. The resulting cell
215 monolayer was scratched with a 200 µL pipette tip generating two parallel
216 wounds and returned to a humidified incubator at 37 °C 5% CO_2. Two replicates
217 for each treatment and four phase-contrast images were acquired along the
218 length of each wound every 2-4 h under 40x magnifications. Cell migration was
219 also assessed in a 96-well format using ORIS cell migration assay from Platypus
220 Technologies (cat. no. CMA1.101). Cells were seeded at a density of $7x10^4$
221 cells/well in 100 µl of medium around the stoppers and left to attach for 24 h.
222 Next day, the stoppers were removed, and phase-contrast images were
223 acquired from each well every 2-4 h. The wound area was determined from
224 these images after delineating the edges digitally using Adobe Photoshop CS4
225 software.

226

227 **Statistical analysis**

228 Data is presented as average ± SD. All experiments were performed in triplicates.
229 Statistical analyses were conducted using GraphPad Prism 7 (GraphPad
230 Software). The statistical test used is indicated in the respective figure legend. $P < 0.05$ was considered as statistically significant.

231

232

Results

The overexpression of PI3KC2β changes the migration front of A431

To further study the implication of PI3KC2β in regulating cell migration (14,21), stably transfected A431 cells were used. First, *PIK3C2B* overexpression was validated at the protein level. Results of the conducted western blots indicated strong PI3KC2β overexpression in stably expressing clones, increasing the levels of this kinase to 233.88 ±16.95% of the parental cell line expression level (Fig 1A). We then tested the effect of this overexpression in terms of cellular migration. The PI3KC2β overexpressing cells presented increase in wound healing closure speed compared to the parental cell line A431 (Fig 1B). During these migration assays, A431 cells appeared to have tighter cell-to-cell junctions, typical from epithelial cells, whereas A431C2β showed a more fibroblastic spindle-like morphology (Fig 1C).

PI3KC2β overexpression increases EMT markers expression.

Following the primary observation, the levels of EMT markers in A431 and A431C2β cells were evaluated. E-cadherin and β-catenin expression were reduced in A431C2β cells compared to A431 by 21% and 71% respectively (Fig 2A). Snail and Twist, two transcription factors involved in EMT presented elevated transcription with almost 4 folds for *SNAI1* and more than 3 folds for *TWIST1* (Fig 2B) of the parental transcription levels in the A431C2β. Finally, immunostaining of Vimentin (green) showed a higher positivity index (more than 7 folds higher) in A431C2β compared to A431 (fig 2C).

256

257 **Cytoplasmic co-localization of E-Cadherin, β-Catenin in A431C2β**

258 To study further the effect of PI3KC2β overexpression, the cellular localizations
259 of E-cadherin and β-catenin were visualized by confocal microscopy after
260 immunofluorescence staining. While in A431 cells, E-cadherin and β-catenin
261 showed staining mainly at the plasma membrane, A431C2β cells, showed
262 staining at both the plasma membrane and in a cytoplasmic region close to the
263 nucleus (Fig 3A).

264 To better define the cytosolic sub compartment of the cell where E-
265 cadherin and β-catenin were localized, dual-color immunofluorescence stainings
266 of β-catenin with either 58K (22) used as a marker of the Golgi apparatus (Fig
267 3B) or Rab 7 (23) as a marker for late endosomes (Fig 3C) were performed. β-
268 catenin co-localized with neither 58K nor Rab 7.

269

270 **Cytoplasmic co-localization of PI3KC2β and EGFR with E-cadherin/β-**
271 **catenin aggregates**

272 In attempt to explain the effect of PI3KC2β-induced cytoplasmic localization of E-
273 cadherin and β-catenin, we tested if PI3KC2β localization was overlapping with
274 E-cadherin and β-catenin. Dual-colour immunofluorescence staining of PI3KC2β
275 with E-Cadherin was also performed revealed partial co-localization of these
276 proteins in the cytoplasm (Fig 4A).

277 We performed here a dual-color immunofluorescence staining of EGFR
278 with E-cadherin (Fig 4B). The overlap of the two signals in the cytoplasm showed

that the two proteins co-localize suggesting that PI3KC2β overexpression is leading to the internalization of E-cadherin, β-catenin and EGFR together in the same intracellular compartment.

PI3KC2β overexpression reduces EGFR signaling

The PI3KC2β-driven relocalization of EGFR has been further examined. Quantitative PCR analysis showed a significant reduction of *EGFR* transcription (-88.47 ±18.87%) but also a significant reduction of EGFR expression (-81.38 ±7.42%) in the A431C2β cells (Fig 5A and 5B) compared to the parental cell line A431. Consequently, alterations in EGFR downstream signaling were analyzed. We could find that A431C2β cells showed decreased phosphorylation levels for AKT (29.81 ±0.69%) and ERK (22.68 ±4.72%) (Fig 5C) compared to their respective total expression. This reduction was less remarkable when compared to beta-Actin, since a strong increase of total-ERK was also found (Fig 5C).

PI3KC2β has also been suggested to participate in chemo-resistance to different drugs (6–8). We therefore tested if this PI3KC2β-driven relocalization of EGFR translates into modified response to EGFR kinase inhibitors. Cell proliferation of the two lines, A431 and A431C2β, was measured after 72 h of treatment with 0.1% DMSO or with increasing concentrations of EGFR kinase inhibitors, Erlotinib and Gefitinib. Results obtained from the crystal violet assay showed that PI3KC2β overexpression increases Erlotinib and Gefitinib resistance (Fig 5D). More specifically, the measured IC50 for Erlotinib shifted from 0.652 µM to 4.434 µM between A431 and A431C2β, and the measured IC50 for Gefitinib shifted from 0.084 µM to 0.47 µM.

The overexpression of PI3KC2β induces also EMT markers expression in HT29 cells

To confirm our observations, HT29 cells were stably transfected with the same Myc-tagged *PIK3C2B* expression vector used for the A431 cells. After transfection, the different generated clones were evaluated on a transcriptional level for *PIK3C2B* overexpression. The clone HT29C2β (1/14) was selected for its highest expression of *PIK3C2B* with a relative expression of 751 ±81.96% in comparisons to the parental HT29 cell line (Fig 7A) or the cells transfected with the empty pcDNA3 vector. The levels of different EMT markers were also evaluated by western blot. In HT29 cells *PIK3C2B* overexpression resulted in a decrease in the expression levels of E-cadherin (-40.05 ±8.62%) in relation to the parental HT29 cell line (Fig 6A). Furthermore, HT29C2β cells also showed increased mRNA levels for *SNAI1* (2.5 folds) (Fig 6B). Finally, the comparison of the morphology of the migration front between HT29 and HT29C2β cells showed in HT29 an apparent tighter cell-to-cell contacts than in HT29C2β (Fig 6C).

Discussion

In this study, we have confirmed that PI3KC2β overexpression in A431 epidermoid carcinoma cells is promoting a more motile phenotype increasing wound healing closured (Fig 1B). Katso *et al.* previously reported that the increased expression of PI3KC2β stimulates Rac activity in these cancer cells, increasing membrane ruffling and migration speed of the cells (14). Moreover, the overexpression of this PI3KC2β also renders A431 cells resistant to anoikis (14). Additionally, in the present study we have observed a change in the

morphology of the cells from the migration front, that switch from apparently tight cell-to-cell contact to a more fibroblastic spindle-like morphology after PI3KC2β overexpression (Fig 1C). This morphology change resembles the cytoskeleton reorganization typical of a EMT process (24,25).

We observed that the overexpression of PI3KC2β induced an increased expression of different EMT markers: mRNA levels of Snail and Twist, increase positivity index of Vimentin and decreased protein levels of E-cadherin and β-catenin (Fig 2). This is consistent with what has been already observed, in prostate cancer that PI3KC2β has been reported to control cell invasion by regulating SLUG expression, a transcription factor promoting EMT progression (13). Additionally, in breast cancer cell lines, PI3KC2β regulates cell invasion and activates the transcription factor STAT3, that controls the expression of master EMT transcription factors (12).

In A431, the induction of EMT can be elicited by a chronic EGF treatment that promotes the endocytosis of E-cadherin followed by the dissociation of the E-cadherin/β-catenin complex and the subsequent trans-activation of the β-catenin/lymphoid enhancer factor 1 (LEF-1) pathway (26,27). We are reporting here that PI3KC2β overexpression is promoting a perinuclear localization of E-cadherin, β-catenin and EGFR instead of mainly at the plasma membrane (Fig 3A, 4A). However, we were not able to determinate their specific cytoplasmic localization as they do not co-localize with markers of Golgi apparatus or late endosomes (Fig 3B-C). Despite this, the proximity to late endosomes markers suggest that these molecules could be localized in another type of endosomes. A similar phenotype was observed in A431 after the treatment with lysophosphatidic acid (LPA) (28). In this study E-cadherin and β-catenin were co-

352 localized by immunostaining in a discrete region near the nucleus that was
353 identical to the perinuclear endocytic recycling compartment (ERC). The authors
354 proposed that the ERC may be a site of residence for β-catenin destined to enter
355 the nucleus, and that this accumulation of β-catenin levels in the ERC could
356 effectively affects β-catenin substrate levels available for downstream pathways
357 and being critical for cancer progression (28).

358 In our study, the dual-colour immunofluorescence staining of PI3KC2β
359 with E-Cadherin revealed a partial co-localization of these proteins in a similar
360 discrete perinuclear region (Fig 4A). This supports the hypothesis that PI3KC2β
361 could be promoting the internalization of E-cadherin, β-catenin and EGFR.
362 PI3KC2β is one of the major producers of PI3P in endosomes (29). Moreover, an
363 *in vivo* study performed by Alliouachene *et al.* reported that the reduction of PI3P
364 upon PI3K-C2β inactivation has selectively impact on endosomal trafficking (11),
365 specifically in the maturation of the APPL1-positive very early endosomes.
366 Moreover, in this study they also observed that PI3K-C2β inactivation led to an
367 accumulation of the insulin receptors in these early endosomal
368 compartments. Therefore, we think that the overexpression of PI3KC2β, probably
369 though an increase in PI3P production, is strongly increasing the level of
370 internalization of E-cadherin, β-catenin and EGFR inducing their accumulation
371 possibly in the ERC. This notably decreases the presence of these molecules in
372 the plasma membrane and adherent junctions, consequently affecting the
373 stabilization of cell-cell adhesion and probably leading to EMT (Fig 7) (28).

374 In addition to the observed effect in the cellular localization of EGFR, a
375 decrease in EGFR expression was also reported after PI3KC2β overexpression
376 (Fig 5B). This observation is in agreement with previous studies showing that in

A431 cells specific cellular context, EMT is also associated with a coordinated loss of EGFR (30). Consistency with the decrease of EGFR, the phosphorylation status of AKT and ERK, downstream targets of this receptor, was also decreased (Fig 5C). This reduction was less remarkable when compared to β-Actin levels, since a strong increase of total-ERK was also found (Fig 5C), suggesting in addition a possible compensatory mechanism.

Together with the decrease in EGFR expression, a reduced sensitivity to the Erlotinib and Gefitinib was also observed (Fig 5D). This is in agreement with the transition to a mesenchymal-like phenotype that is known to decrease the cellular dependence on EGFR signalling, as alternative growth pathways are activated (31) (Fig 7). This has been confirmed in different clinical trials where NSCLC with high expression of E-cadherin showed a beneficial response to Erlotinib treatment in comparison to E-cadherin-negative patients who have an overall deteriorated condition (32). Carcinoma cell lines expressing epithelial proteins, such as E-cadherin, are sensitive to growth inhibition by erlotinib, whereas those tumour cell lines that had undergone an EMT-like transition are less sensitive to EGFR inhibition (33). Similar patterns have been reported for pancreatic and colorectal tumour cell lines (34).

Additionally, PI3KC2β has also been suggested to participate in the resistance to different chemotherapeutic compounds like tamoxifen, cisplatin, Etoposide and Doxorubicin (18,19,35). Moreover, PI3KC2β expression has also been significantly correlated to resistance towards Erlotinib in glioblastoma pathogenesis which supports our results (36).

In HT29 cells the stable overexpression of PI3KC2β was able to reproduce the most notable changes observed in A431 cells. HT29C2β showed increased

mRNA levels of Snail and decreased protein levels of E-Cadherin (Fig 6A-B). A change in migration pattern decreasing cell-to-cell contact was also observed in this cancer cell line (Fig 6C). These results further validate our hypothesis where the overexpression of PI3KC2β is promoting EMT.

To conclude, our study shows a link between the overexpression of PI3KC2β, the regulation of intracellular vesicular trafficking and EMT. Further studies are needed to test PI3KC2β as a drug target to revert this malignant phenotype and prevent metastasis formation. Moreover, there is still a necessity to clarify the signalling pathways specifically regulated by PI3KC2β because the recompilation of previous studies suggest that it could be cell/tissue specific. For example, while in some cancers AKT has been proposed as a downstream target (18,19,37), in others this lipid kinase has been associated with MAPK signalling pathway (13), or an alternative miR-449a/β-catenin/cyclin B1 pathway (12). Therefore, the implication of PI3KC2β in EMT could variate depending on the cellular context, and this makes urgent further studies to understand the specific role of this lipid kinase in human biology and tumorigenesis.

Acknowledgments

We would like to acknowledge the Microscopy Imaging Center of the University of Bern (MIC). Dr Silvia Crespo was enrolled in the Graduate School for Cellular and Biomedical Sciences (GCB) of the University of Bern during the work presented here, we would like therefore to acknowledge it for the training provided. We would also like to thank Dr. Karolina Blajecka for providing the

HT29C2β cells and Prof J. Gertsch for his support during the thesis work. We would also like to acknowledge the financial support of the Berner Stiftung für krebskranke Kinder und Jugendliche as well as Batzebär.

References

1. Di Paolo G, De Camilli P. Phosphoinositides in cell regulation and membrane dynamics. Nature. 2006 Oct;443(7112):651–7.

2. Vanhaesebroeck B, Guillermet-Guibert J, Graupera M, Bilanges B. The emerging mechanisms of isoform-specific PI3K signalling. Nat Rev Mol Cell Biol. 2010 May;11(5):329–41.

3. Samuels Y, Ericson K. Oncogenic PI3K and its role in cancer. Curr Opin Oncol. 2006 Jan;18(1):77–82.

4. MacDougall LK, Domin J, Waterfield MD. A family of phosphoinositide 3-kinases in Drosophila identifies a new mediator of signal transduction. Curr Biol. 1995 Dec;5(12):1404–15.

5. Virbasius J V, Guilherme A, Czech MP. Mouse p170 is a novel phosphatidylinositol 3-kinase containing a C2 domain. J Biol Chem. 1996 Jun;271(23):13304–7.

6. Arcaro A, Volinia S, Zvelebil MJ, Stein R, Watton SJ, Layton MJ, et al. Human phosphoinositide 3-kinase C2beta, the role of calcium and the C2 domain in enzyme activity. J Biol Chem. 1998 Dec;273(49):33082–90.

7. Brown RA, Ho LKF, Weber-Hall SJ, Shipley JM, Fry MJ. Identification and cDNA Cloning of a Novel Mammalian C2 Domain-Containing Phosphoinositide 3-Kinase, HsC2-PI3K. Biochem Biophys Res Commun. 1997 Apr;233(2):537–44.

8. Arcaro A, Zvelebil MJ, Wallasch C, Ullrich A, Waterfield MD, Domin J. Class II phosphoinositide 3-kinases are downstream targets of activated polypeptide growth factor receptors. Mol Cell Biol. American Society for Microbiology (ASM);

2000 Jun;20(11):3817–30.

9. Maffucci T, Cooke FT, Foster FM, Traer CJ, Fry MJ, Falasca M. Class II phosphoinositide 3-kinase defines a novel signaling pathway in cell migration. J Cell Biol. 2005;169(5).

10. Falasca M, Maffucci T. Rethinking phosphatidylinositol 3-monophosphate. Biochim Biophys Acta - Mol Cell Res. 2009 Dec;1793(12):1795–803.

11. Alliouachene S, Bilanges B, Chicanne G, Anderson KE, Pearce W, Ali K, et al. Inactivation of the Class II PI3K-C2β Potentiates Insulin Signaling and Sensitivity. Cell Rep. 2015;13(9):1881–94.

12. Chikh A, Ferro R, Abbott JJ, Piñeiro R, Buus R, Iezzi M, et al. Class II phosphoinositide 3-kinase C2β regulates a novel signaling pathway involved in breast cancer progression. Oncotarget. 2016;7(14):18325–45.

13. Mavrommati I, Cisse O, Falasca M, Maffucci T. Novel roles for class II Phosphoinositide 3-Kinase C2β in signalling pathways involved in prostate cancer cell invasion. Sci Rep. Nature Publishing Group; 2016;6(MARCH):23277.

14. Katso RM, Pardo OE, Palamidessi A, Franz CM, Marinov M, De Laurentiis A, et al. Phosphoinositide 3-Kinase C2beta regulates cytoskeletal organization and cell migration via Rac-dependent mechanisms. Mol Biol Cell. American Society for Cell Biology; 2006 Sep;17(9):3729–44.

15. Srivastava S, Di L, Zhdanova O, Li Z, Vardhana S, Wan Q, et al. The class II phosphatidylinositol 3 kinase C2beta is required for the activation of the K+ channel KCa3.1 and CD4 T-cells. Mol Biol Cell. American Society for Cell Biology; 2009 Sep;20(17):3783–91.

16. Sato N, Fukushima N, Maitra A, Iacobuzio-Donahue CA, van Heek NT, Cameron JL, et al. Gene Expression Profiling Identifies Genes Associated with Invasive Intraductal Papillary Mucinous Neoplasms of the Pancreas. Am J Pathol. 2004 Mar;164(3):903–14.

17. Boller D, Doepfner KT, De Laurentiis A, Guerreiro AS, Marinov M, Shalaby T, et

al. Targeting PI3KC2beta impairs proliferation and survival in acute leukemia, brain tumours and neuroendocrine tumours. Anticancer Res. 2012;32(8):3015–27.

18. Boller D, Doepfner KT, De Laurentiis A, Guerreiro AS, Marinov M, Shalaby T, et al. Targeting PI3KC2β impairs proliferation and survival in acute leukemia, brain tumours and neuroendocrine tumours. Anticancer Res. 2012 Aug;32(8):3015–27.

19. Liu Z, Sun C, Zhang Y, Ji Z, Yang G. Phosphatidylinositol 3-Kinase-C2$β$ Inhibits Cisplatin-Mediated Apoptosis via the Akt Pathway in Oesophageal Squamous Cell Carcinoma. J Int Med Res. 2011 Aug;39(4):1319–32.

20. Peinado H, Ballestar E, Esteller M, Cano A. Snail mediates E-cadherin repression by the recruitment of the Sin3A/histone deacetylase 1 (HDAC1)/HDAC2 complex. Mol Cell Biol. American Society for Microbiology; 2004 Jan;24(1):306–19.

21. Domin J, Harper L, Aubyn D, Wheeler M, Florey O, Haskard D, et al. The class II phosphoinositide 3-kinase PI3K-C2β regulates cell migration by a PtdIns(3)P dependent mechanism. J Cell Physiol. 2005 Dec;205(3):452–62.

22. Bloom G, Brashear TA. A Novel 58- , kDa Protein Associates with the Golgi Apparatus and Microtubules *. 1989;264(27):16083–92.

23. Feng Y, Press B, Wandinger-Ness A. Rab 7: an important regulator of late endocytic membrane traffic. J Cell Biol. 1995 Dec;131(6 Pt 1):1435–52.

24. Wheelock MJ, Shintani Y, Maeda M, Fukumoto Y, Johnson KR. Cadherin switching. J Cell Sci. 2008 Feb;121(6):727–35.

25. Yilmaz M, Christofori G. Mechanisms of Motility in Metastasizing Cells. Mol Cancer Res. 2010 May;8(5):629–42.

26. Peinado H, Olmeda D, Cano A. Snail, Zeb and bHLH factors in tumour progression: an alliance against the epithelial phenotype? Nat Rev Cancer. 2007 Jun;7(6):415–28.

510 27. Lu Z, Ghosh S, Wang Z, Hunter T. Downregulation of caveolin-1 function by EGF
511 leads to the loss of E-cadherin, increased transcriptional activity of beta-catenin,
512 and enhanced tumor cell invasion. Cancer Cell. 2003 Dec;4(6):499–515.

513 28. Kam Y, Quaranta V. Cadherin-bound beta-catenin feeds into the Wnt pathway
514 upon adherens junctions dissociation: evidence for an intersection between
515 beta-catenin pools. PLoS One. Public Library of Science; 2009;4(2):e4580.

516 29. Marat AL, Haucke V. Phosphatidylinositol 3-phosphates-at the interface
517 between cell signalling and membrane traffic. EMBO J. European Molecular
518 Biology Organization; 2016 Mar;35(6):561–79.

519 30. Thiery JP. Epithelial–mesenchymal transitions in tumour progression. Nat Rev
520 Cancer. 2002 Jun;2(6):442–54.

521 31. Barr S, Thomson S, Buck E, Russo S, Petti F, Sujka-Kwok I, et al. Bypassing cellular
522 EGF receptor dependence through epithelial-to-mesenchymal-like transitions.
523 Clin Exp Metastasis. Springer Netherlands; 2008 Oct;25(6):685–93.

524 32. Voulgari A, Pintzas A. Epithelial?mesenchymal transition in cancer metastasis:
525 Mechanisms, markers and strategies to overcome drug resistance in the clinic.
526 Biochim Biophys Acta - Rev Cancer. 2009 Dec;1796(2):75–90.

527 33. Thomson S, Buck E, Petti F, Griffin G, Brown E, Ramnarine N, et al. Epithelial to
528 Mesenchymal Transition Is a Determinant of Sensitivity of Non–Small-Cell Lung
529 Carcinoma Cell Lines and Xenografts to Epidermal Growth Factor Receptor
530 Inhibition. Cancer Res. 2005;65(20).

531 34. Buck E, Eyzaguirre A, Barr S, Thompson S, Sennello R, Young D, et al. Loss of
532 homotypic cell adhesion by epithelial-mesenchymal transition or mutation limits
533 sensitivity to epidermal growth factor receptor inhibition. Mol Cancer Ther.
534 2007;6(2).

535 35. Iorns E, Lord CJ, Ashworth A. Parallel RNAi and compound screens identify the
536 PDK1 pathway as a target for tamoxifen sensitization. Biochem J. 2009
537 Jan;417(1):361–71.

538 36. Löw S, Vougioukas VI, Hielscher T, Schmidt U, Unterberg A, Halatsch ME.
539 Pathogenetic pathways leading to glioblastoma multiforme: Association
540 between gene expressions and resistance to erlotinib. Anticancer Res. 2008;28(6
541 A):3729–32.

542 37. Russo A, Okur MN, Bosland M, O'Bryan JP. Phosphatidylinositol 3-kinase, class 2
543 beta (PI3KC2β) isoform contributes to neuroblastoma tumorigenesis. Cancer
544 Lett. 2015;359(2):262–8.

545

546

Figure legends

Figure 1: The overexpression of PI3KC2β changes the migration front of A431. A Western blot and Relative protein expression of PI3KC2β in A431 and A431C2β cells. **B** Wound healing closure in A431 and A431C2β cells after 18 h of generating a wound with a 200 µL pipette tip. Images are representative of 4 different experiments performed in a 6 well plate. **C** Comparison of the cell morphology during cell migration of A431 and A431C2β cells in 96 well plates. Representative images obtained through phase-contrast microscopy. Means ±SD; n = 4 independent experiments; unpaired two tailed t-test.

Figure 2: The overexpression of PI3KC2β increases the expression of EMT markers in A431. A Western blot and relative protein expression of E-cadherin and β-catenin in A431 and A431C2β cells. **B** Relative mRNA expression of *SNAI1* and *TWIST1* in A431 and A431C2β cells. **C** Expression of Vimentin visualized by immunofluorescence in A431 and A431C2β cells. Nuclear staining with DAPI (blue) and anti-Vimentin antibody (green). The results of A431C2β were normalized to A431 samples. Means ±SD; n ≥ 3 independent experiments; unpaired two tailed t-test. Size bar = 500µm.

Figure 3: Cytoplasmic co-localization of E-cadherin, β-catenin in A431C2β

Dual-color immunofluorescence co-localization was performed in A431 and A431C2β cells grown on glass coverslips. Images were obtained by confocal

570 microscopy. **A** Expression of E-cadherin (red) and β-catenin (green) visualized
571 with immunofluorescence in A431 and A431C2β cells. **B** Expression of 58K, a
572 golgi marker (red) and β-catenin (green) visualized with immunofluorescence in
573 A431 and A431C2β cells. **C** Expression of Rab7, a late endosome marker (red)
574 and β-catenin (green) visualized with immunofluorescence in A431 and A431C2β
575 cells. Nuclei counterstain with DAPI (blue). Size bar = 50μm.

576

577 **Figure 4: Cytoplasmic co-localization of PI3KC2β and EGFR with E-**
578 **cadherin/β-catenin aggregates.** Dual-color immunofluorescence co-
579 localization was performed in A431 and A431C2β cells grown on glass
580 coverslips. Images were obtained by confocal microscopy. **A** Expression of E-
581 cadherin (red) and PI3KC2β (green) visualized with immunofluorescence in
582 A431C2β cells. **B** Expression of E-cadherin (red) and EGFR (green) visualized
583 with immunofluorescence in A431C2β cells. Nuclei counterstain with DAPI (blue).
584 Size bar = 50μm.

585

586 **Figure 5: The effect of PI3KC2β overexpression in EGFR signalling**

587 *EGFR* transcription (**A**) and EGFR expression (**B**) compared by qPCR and
588 western blots in A431C2β cell line compared to parental cell line. **C** Western blot
589 picture and analyses for EGFR, AKT phosphorylation and ERK phosphorylation
590 in A431 and in A431C2β. **D** A431 and A431C2β, dose response to EGFR TKIs,
591 Erlotinib and Gefitinib. Cell viability was measured via Crystal violet assay. Means
592 ±SD; n = 3 independent experiments; unpaired two tailed t-test.

593

Figure 6: The overexpression of PI3KC2β induces the expression of some EMT markers in HT29. A Relative protein expression of E-cadherin in HT29 cells, HT29 cells transfected with pcDNA3 plasmid, and HT29C2β (clone 1/14) cells transfected with a pcDNA3-PI3KC2β plasmid (evaluated by Western blot). **B** Relative mRNA transcription of *SNAI1* in HT29 and HT29C2β cells (evaluated by qPCR). The results were normalized to HT29 samples. Means ± SD; n ≥ 3 independent experiments; unpaired two tailed t-test. **C** Comparison of the cell morphology during cell migration of HT29 and HT29C2β. Representative images obtained through phase-contrast microscopy.

Figure 7: Proposed model of how the overexpression of PI3KC2β affects intracellular vesicular trafficking of E-cadherin, β-catenin and EGFR and promotes EMT.

Left: Early phase of EMT: PI3KC2β induces the endocytic internalization of EGFR, E-cadherin and β-catenin removing these adherent components and the receptor from cell surface. Additionally, the overexpression of PI3KC2β contribute to the activation of the expression of different transcription factors like Twist and Snail. This constitutes the transcriptional machinery that will lead to EMT.

Right: Late phase of EMT: Twist and Snail will repress the expression of E-cadherin and EGFR. The reduced expression of E-cadherin destabilizes cell-cell adhesions promoting a change in the morphology of the cell.

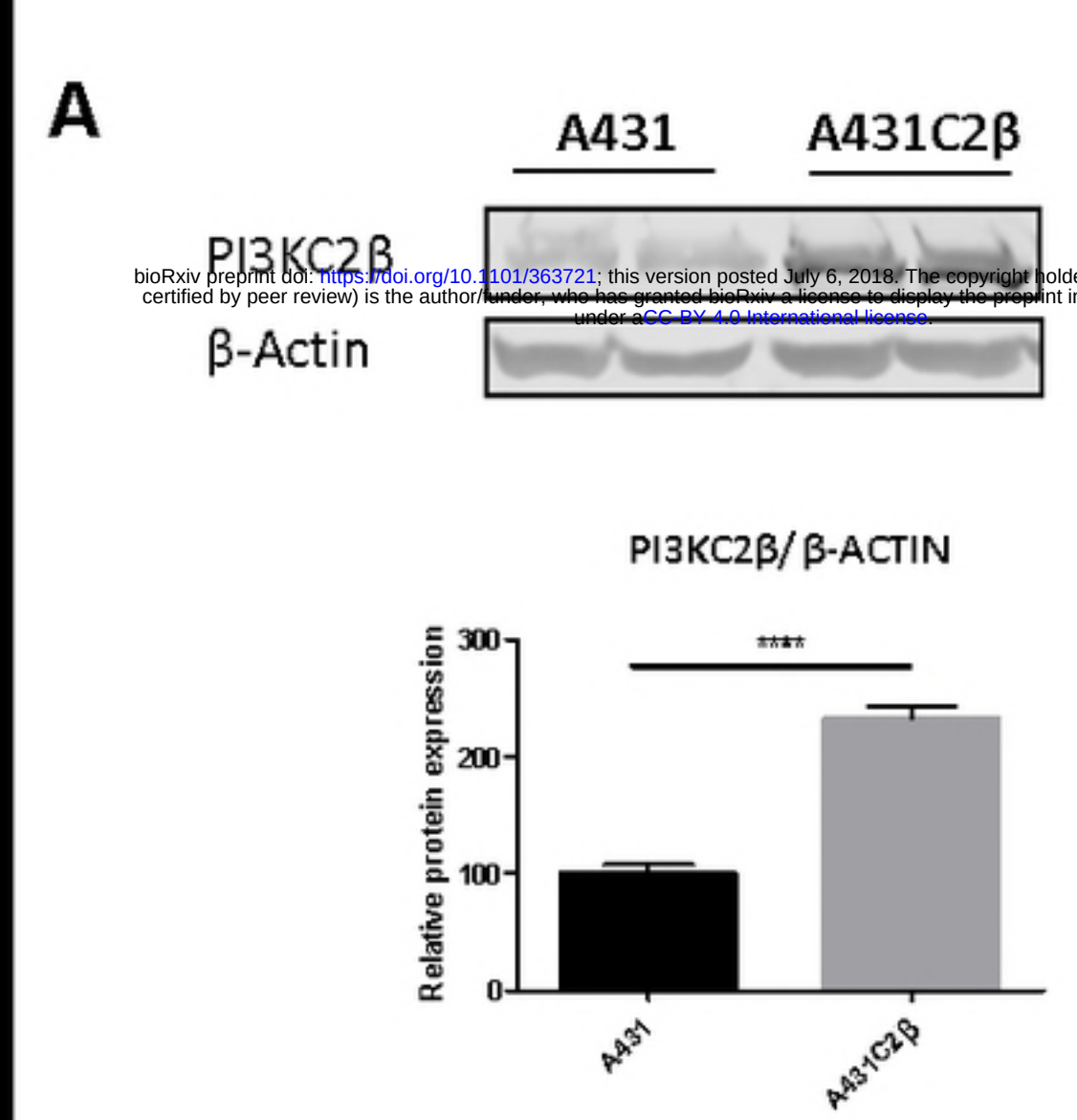

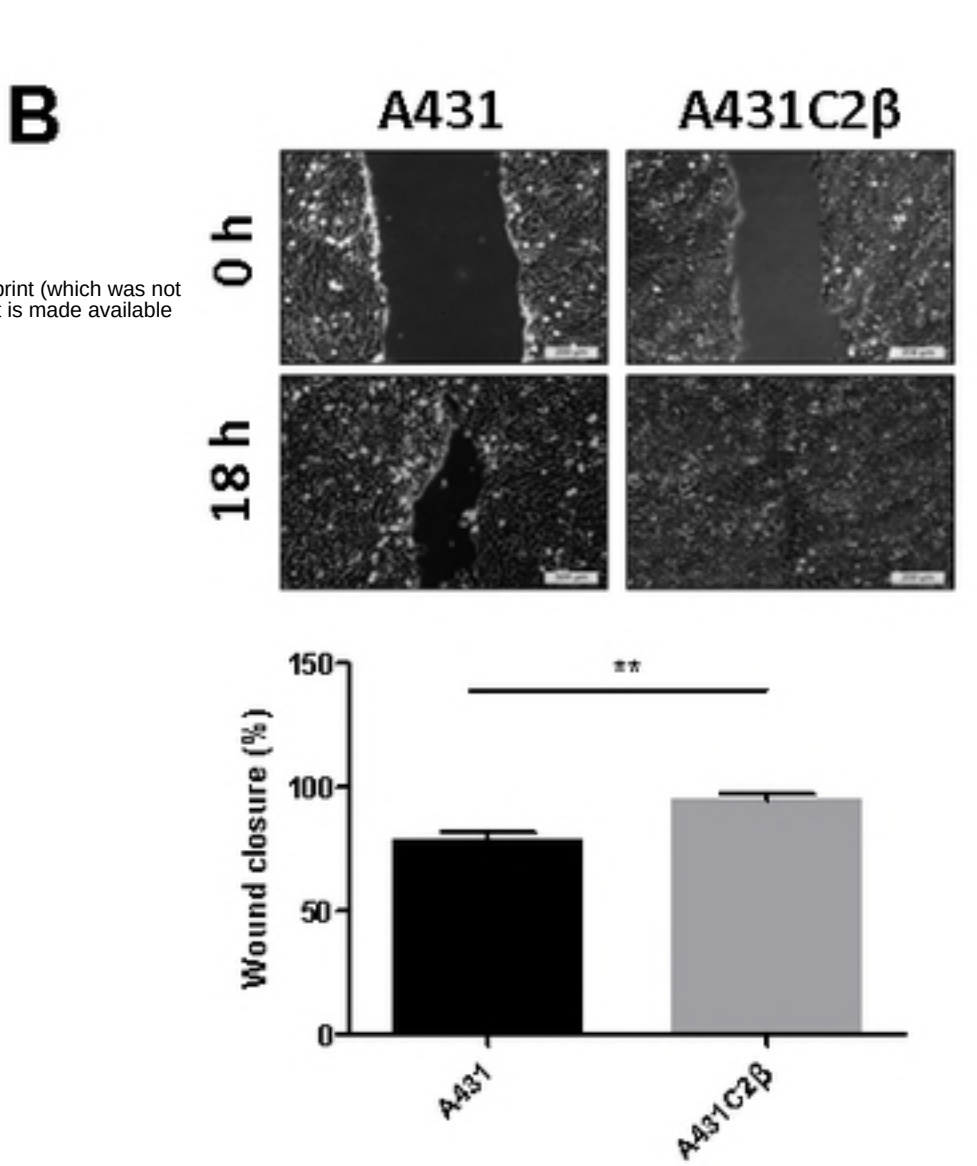

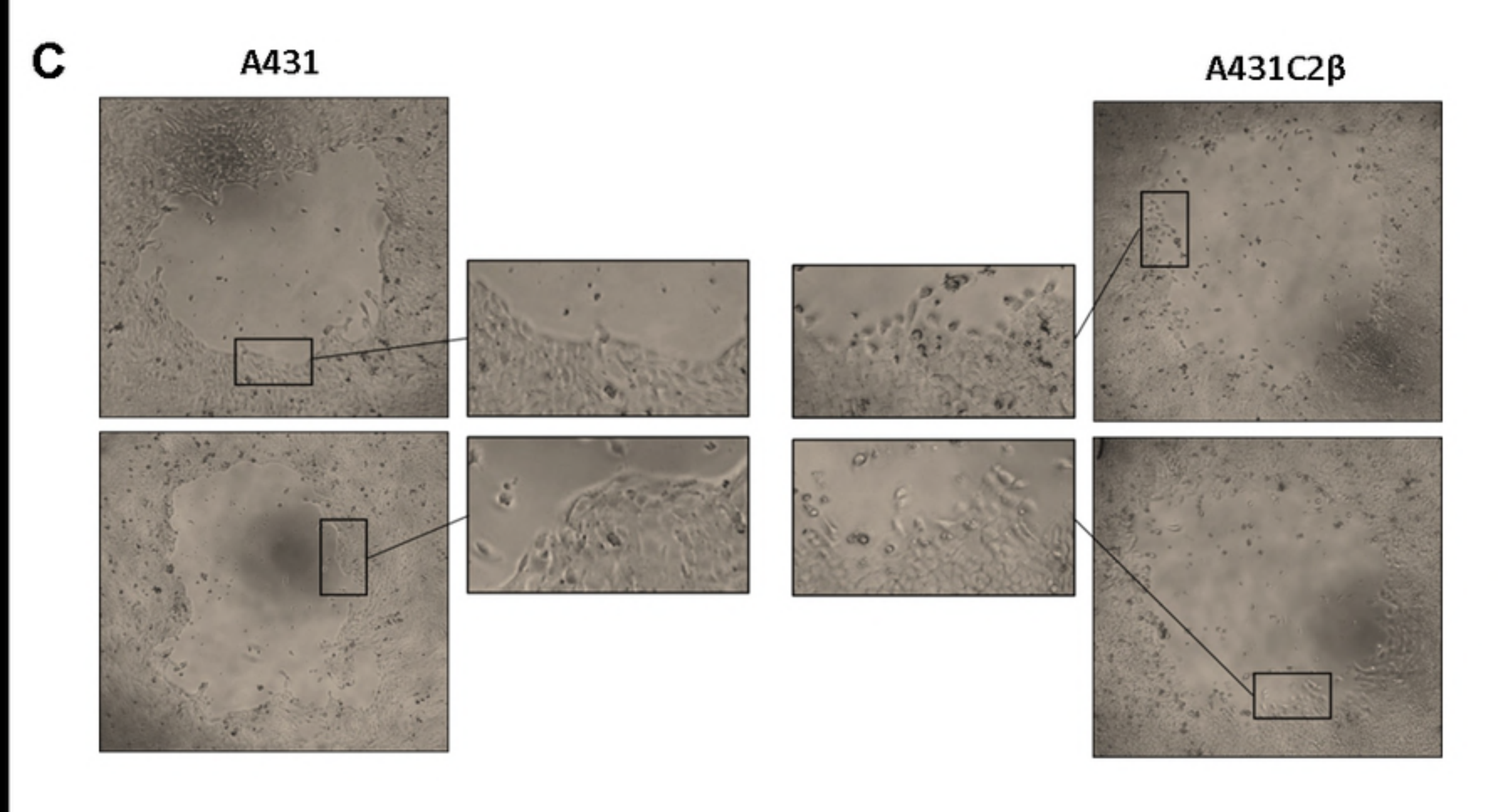

A

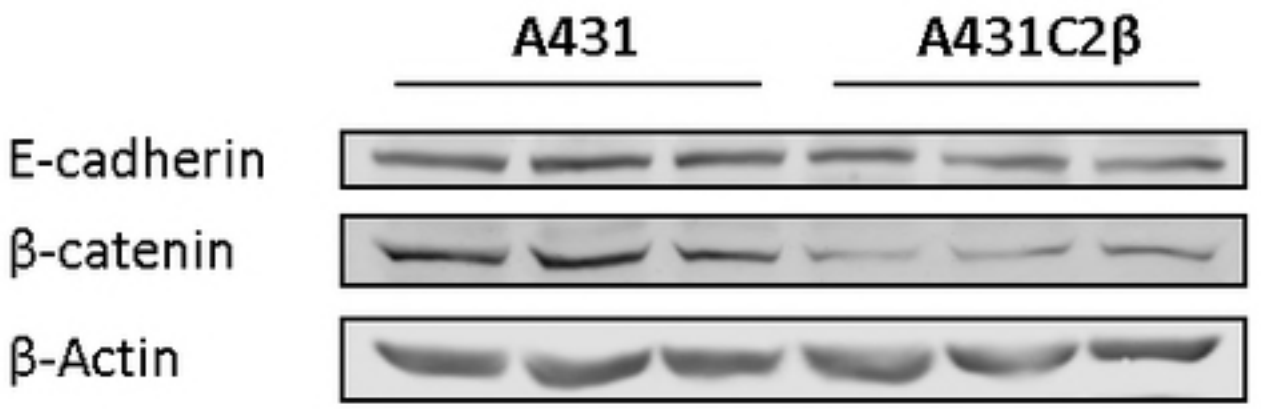

B

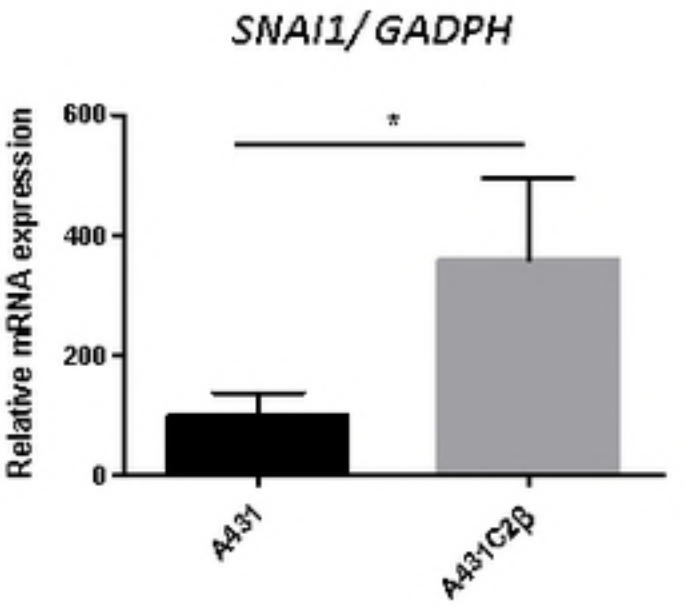

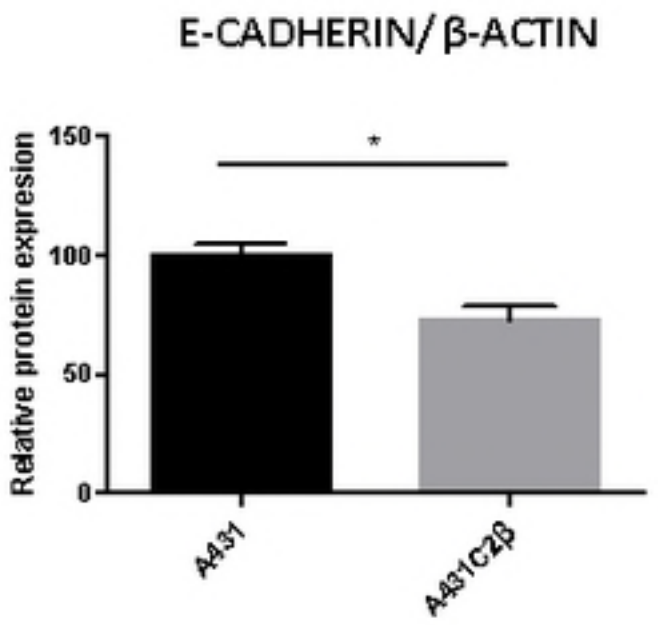

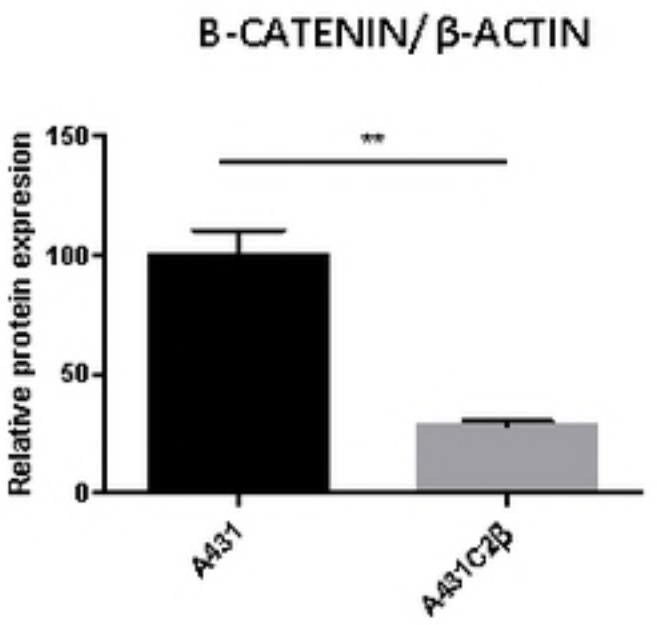

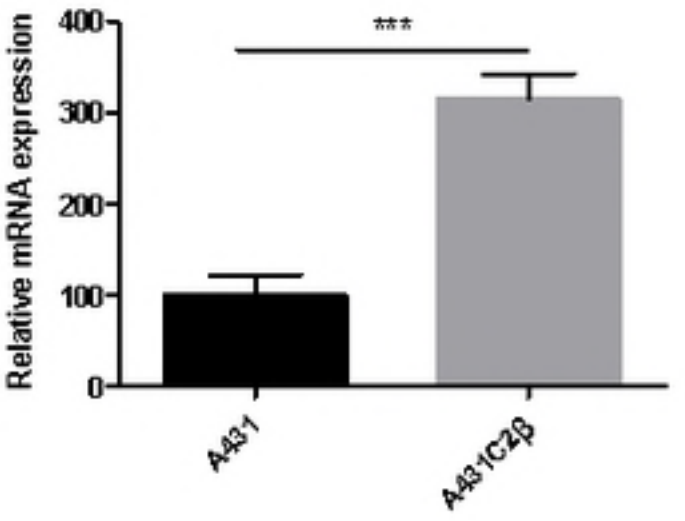

C

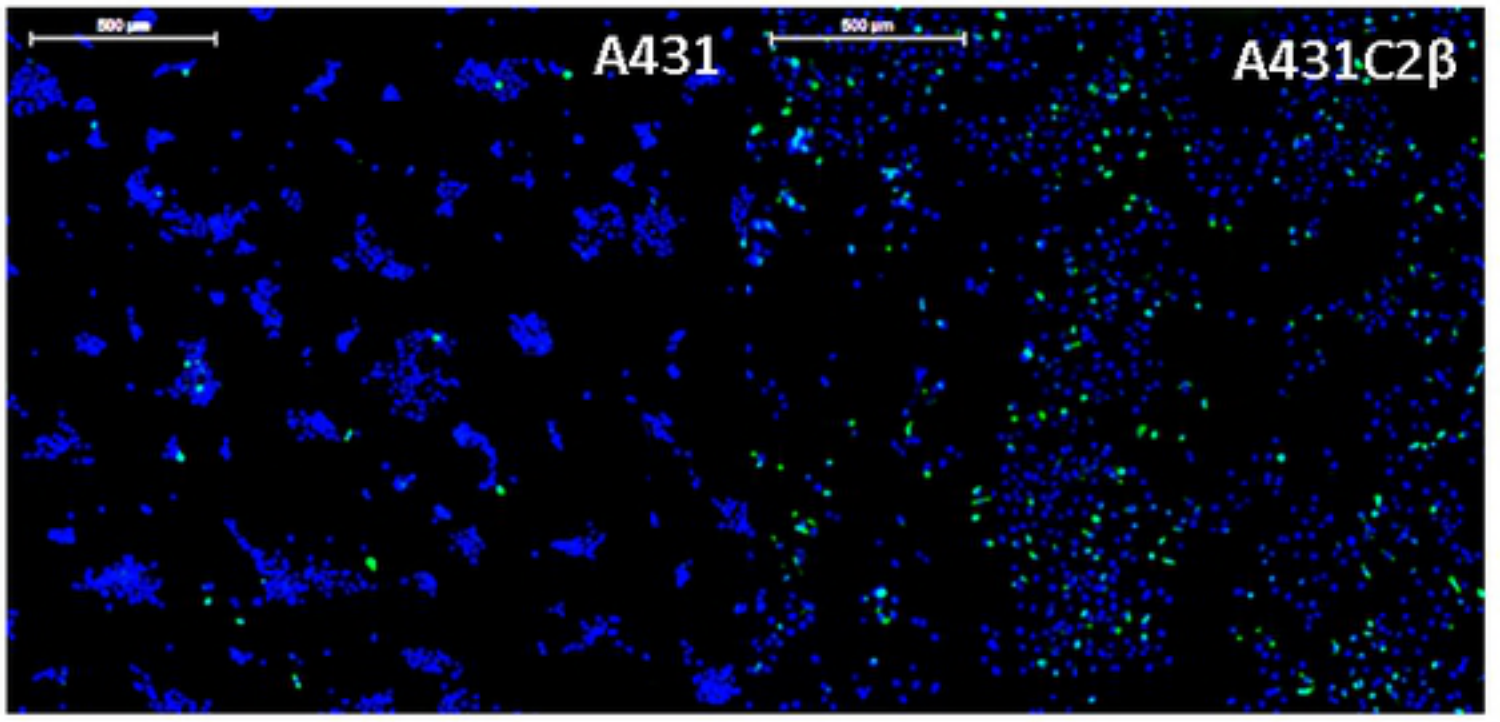

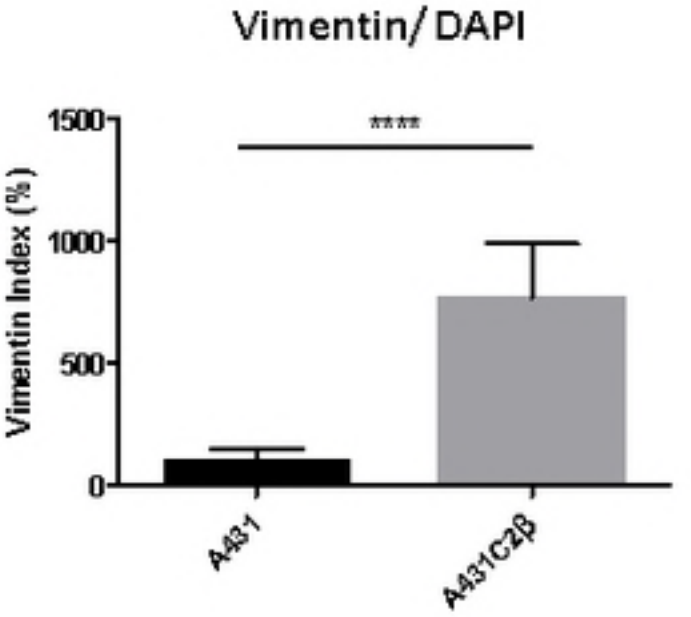

A

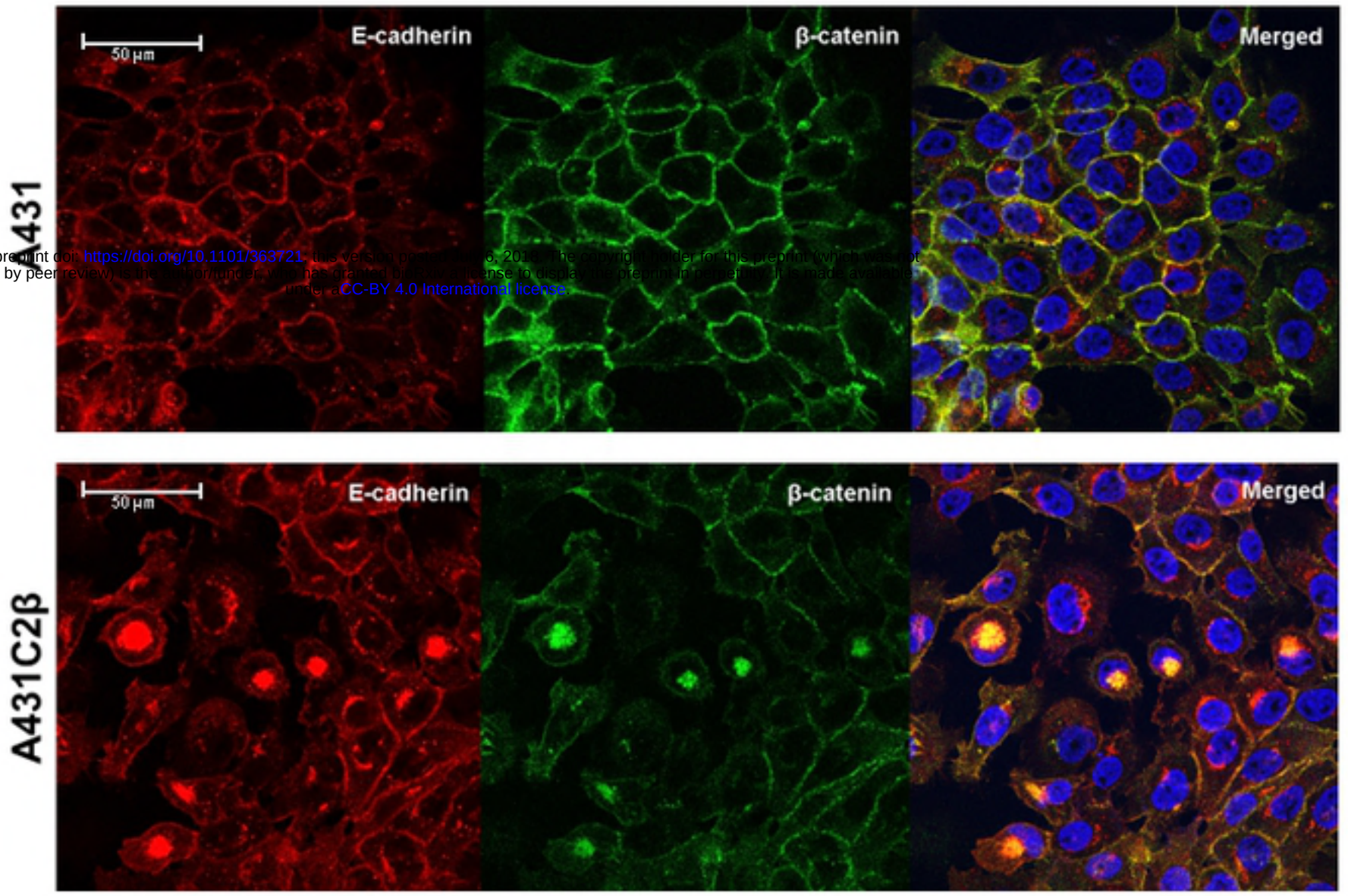

B

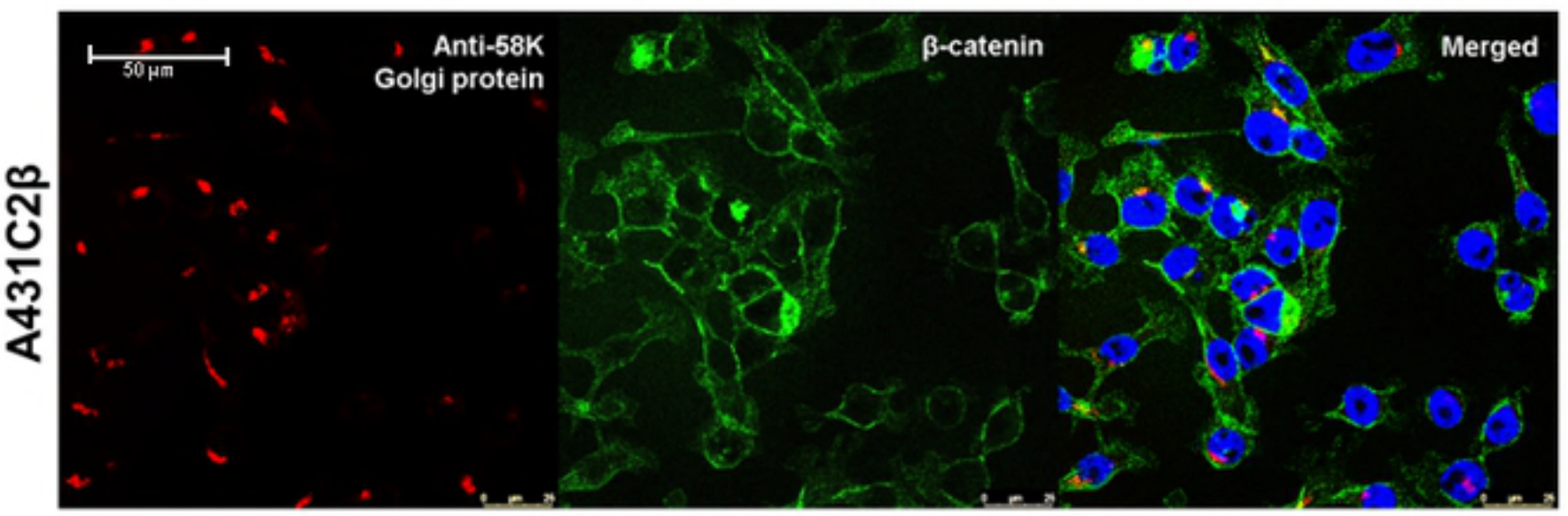

C

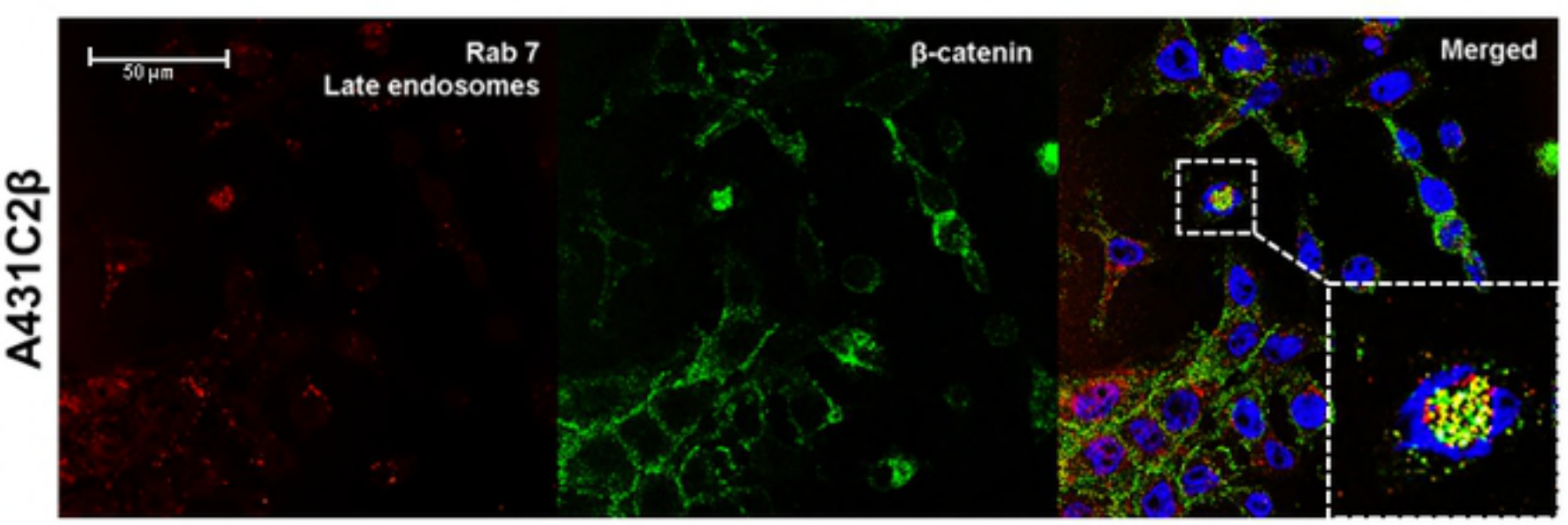

A

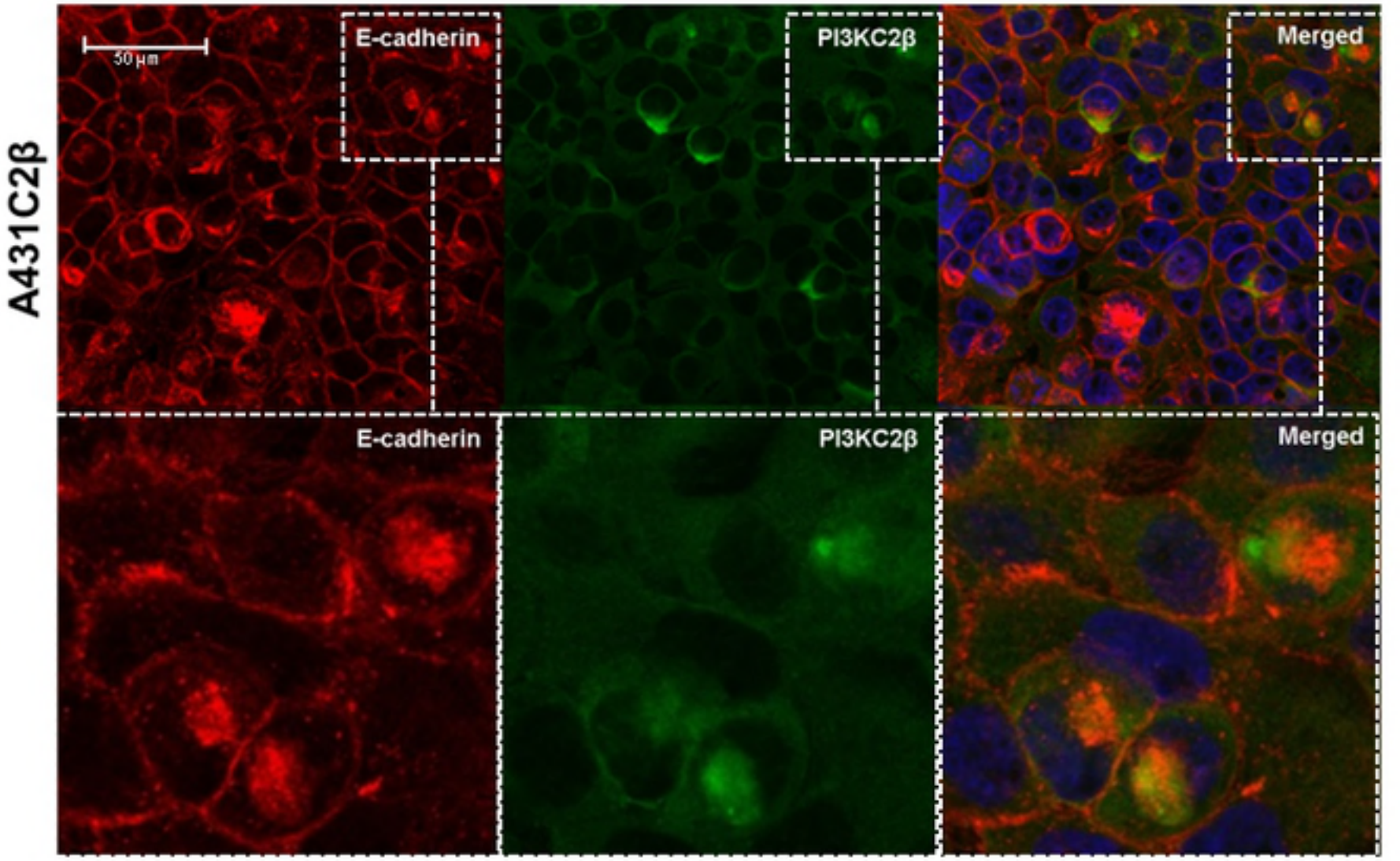
A431C2β
30 μm
E-cadherin
PI3KC2β
Merged
E-cadherin
PI3KC2β
Merged

B

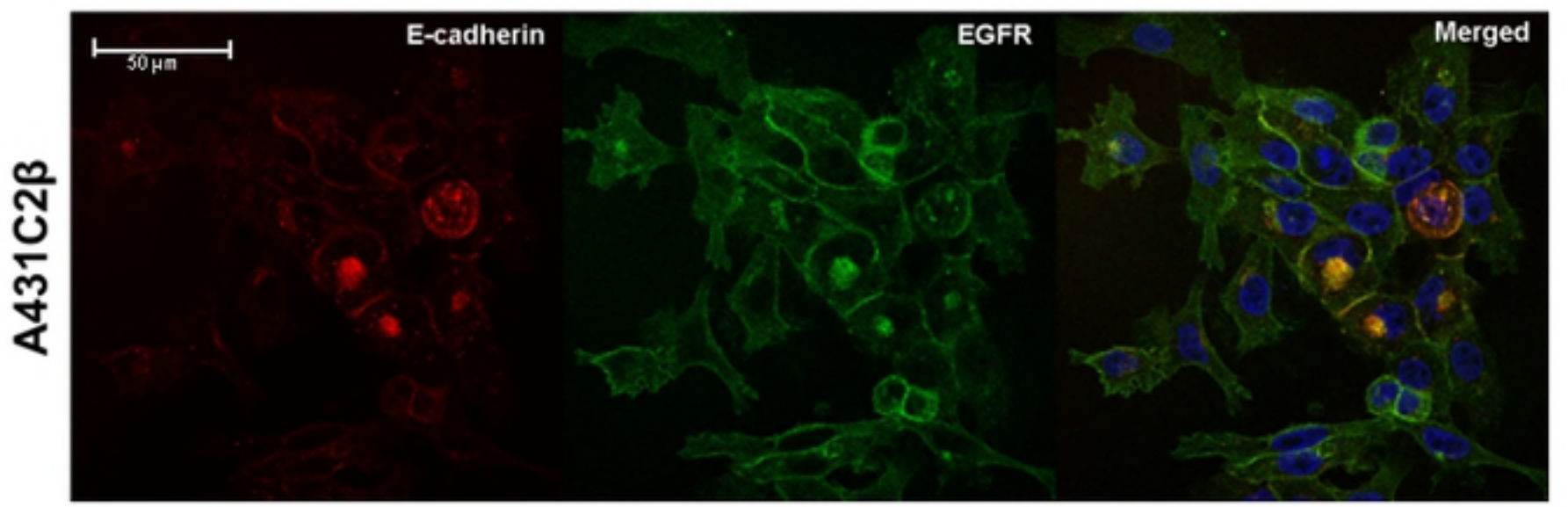
A431C2β
30 μm
E-cadherin
EGFR
Merged

A

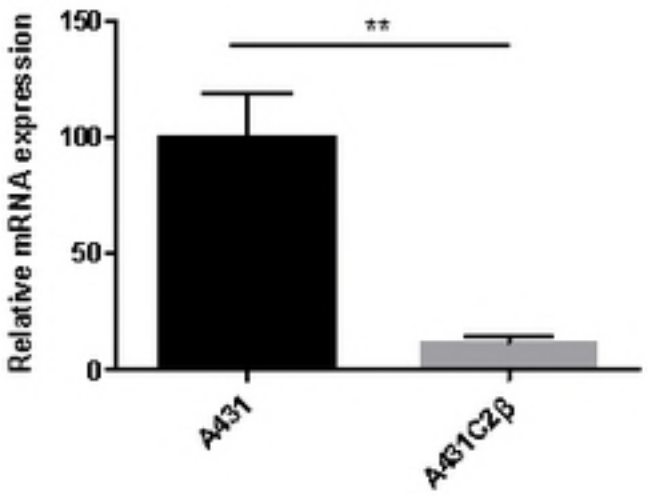

B

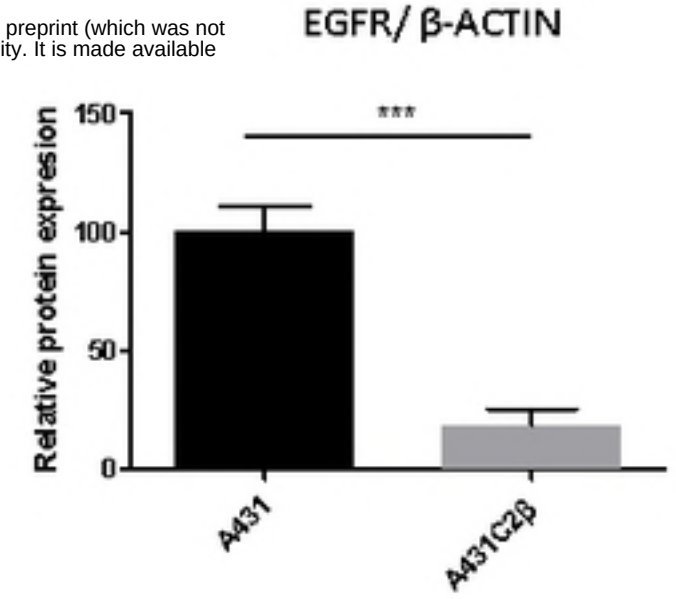

C

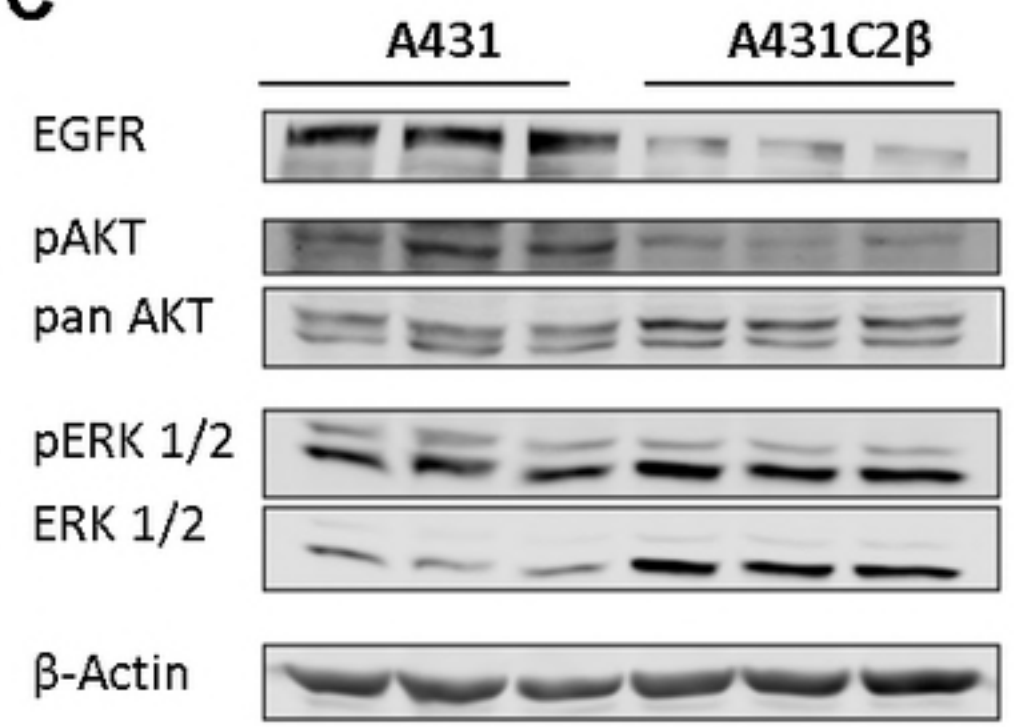

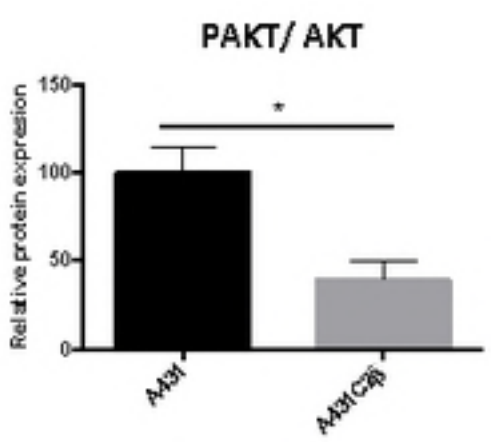

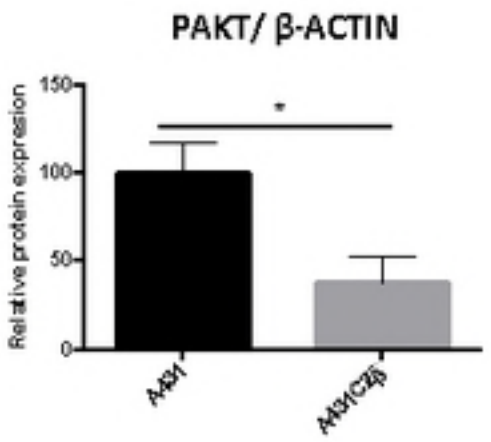

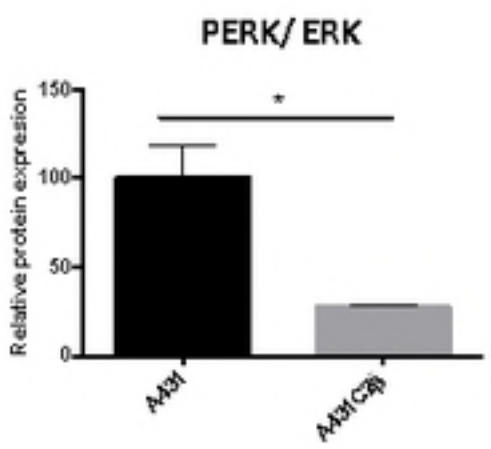

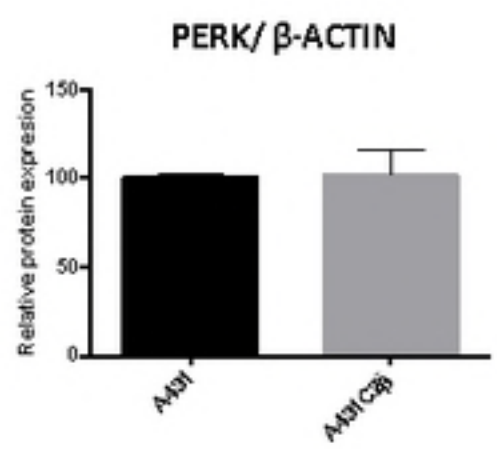

D

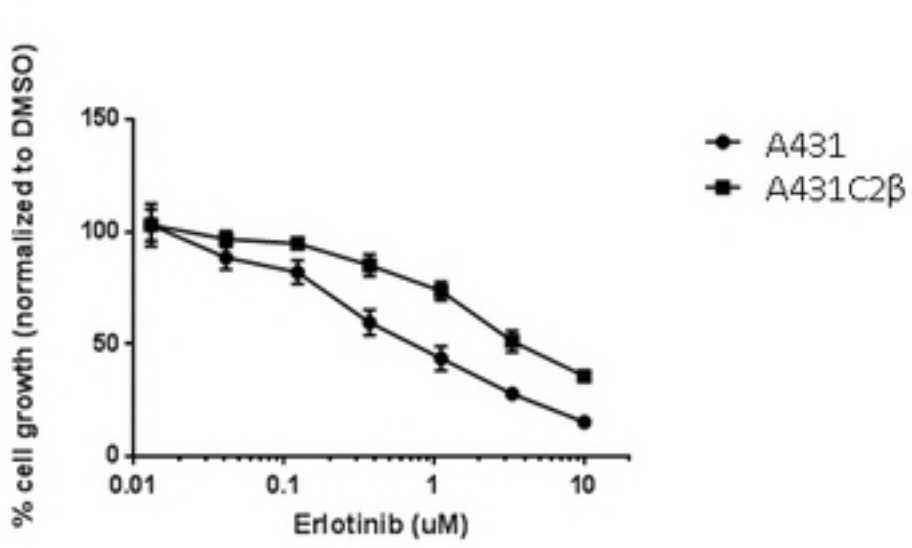

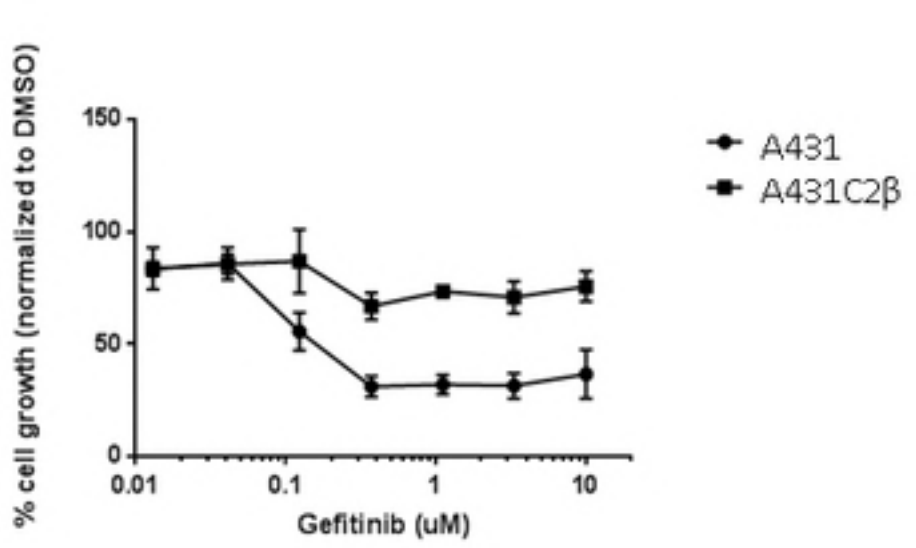

A

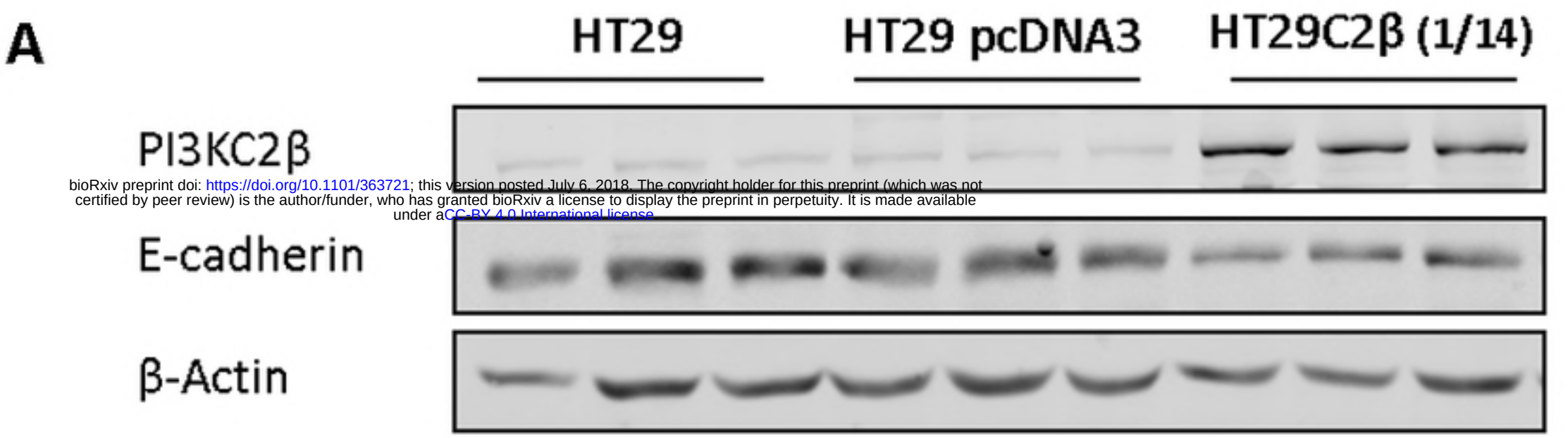

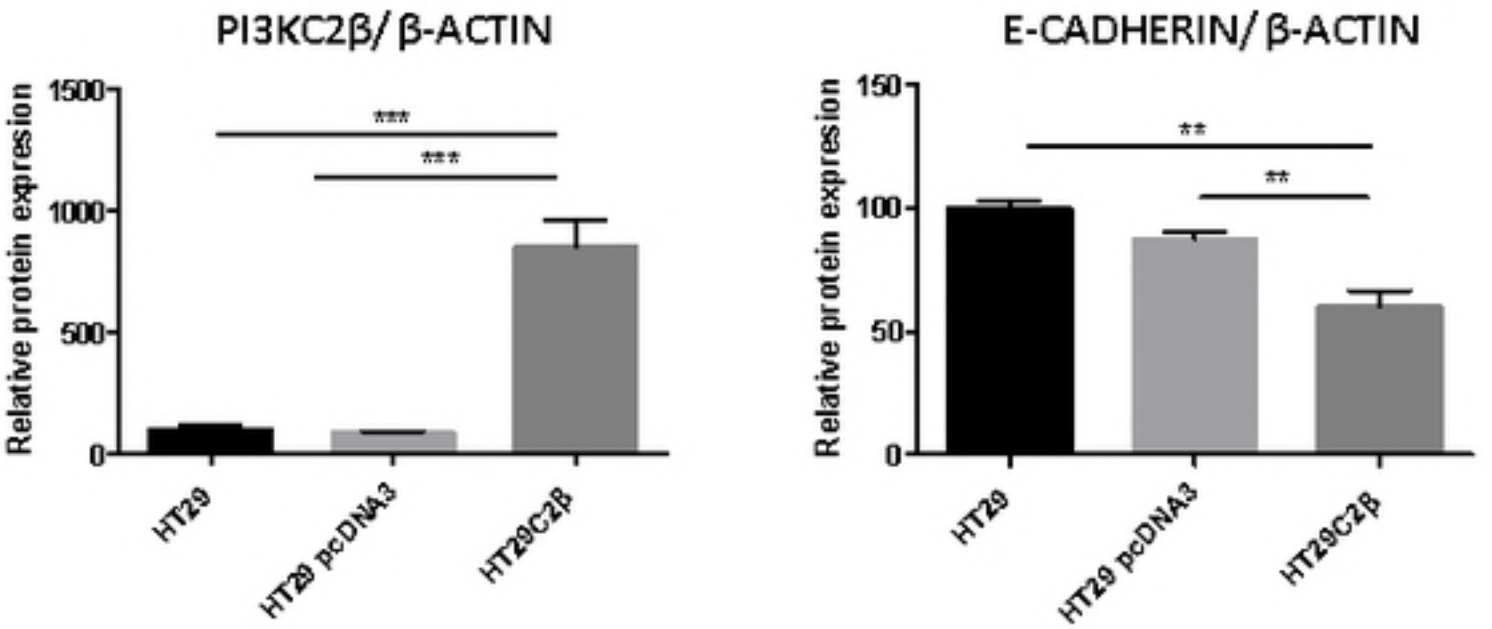

B

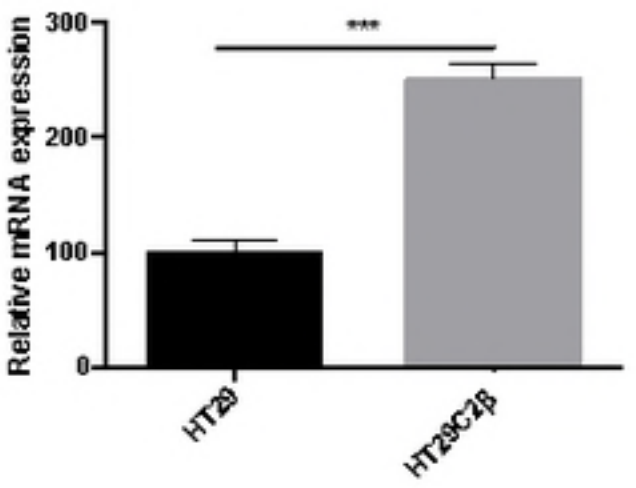

C

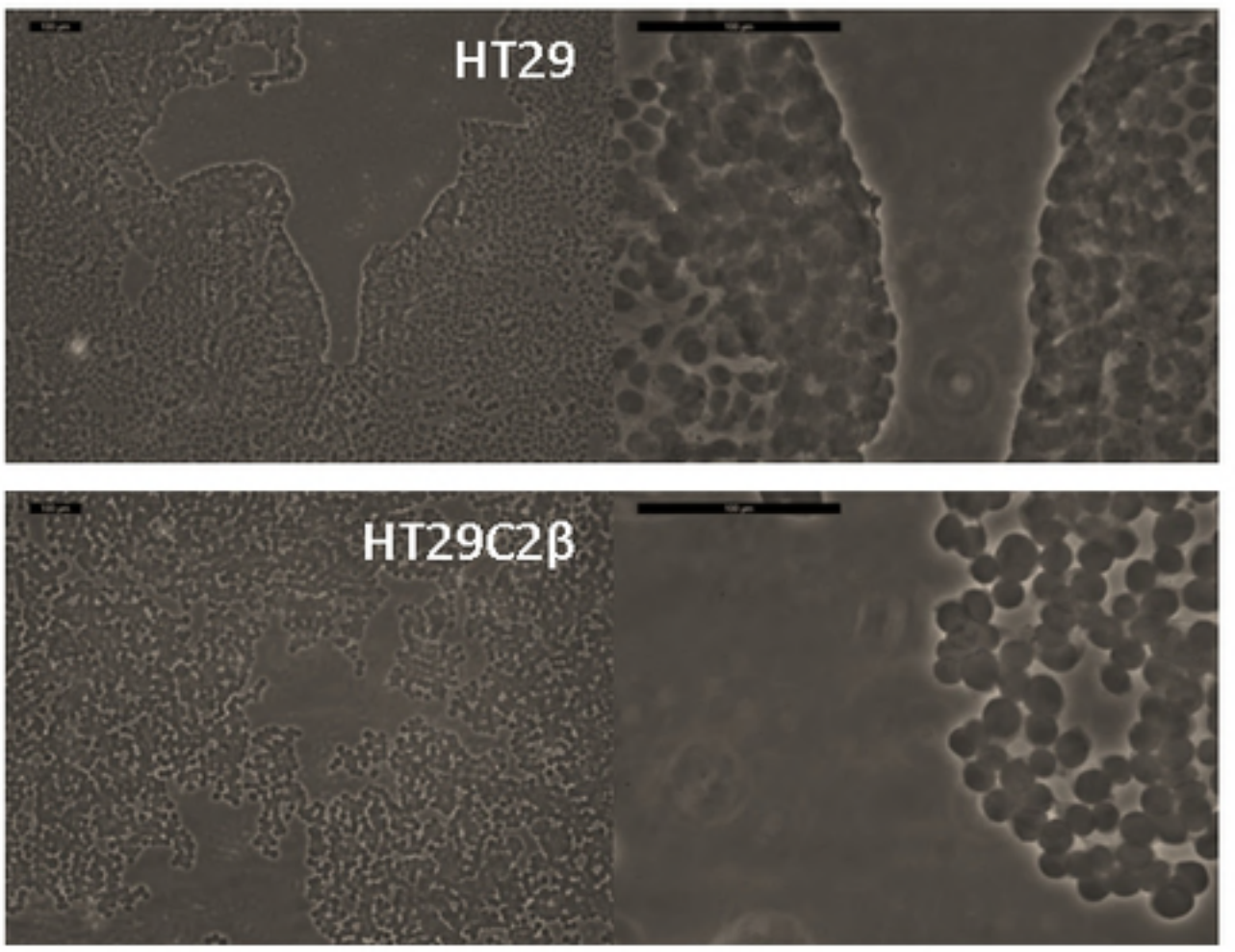

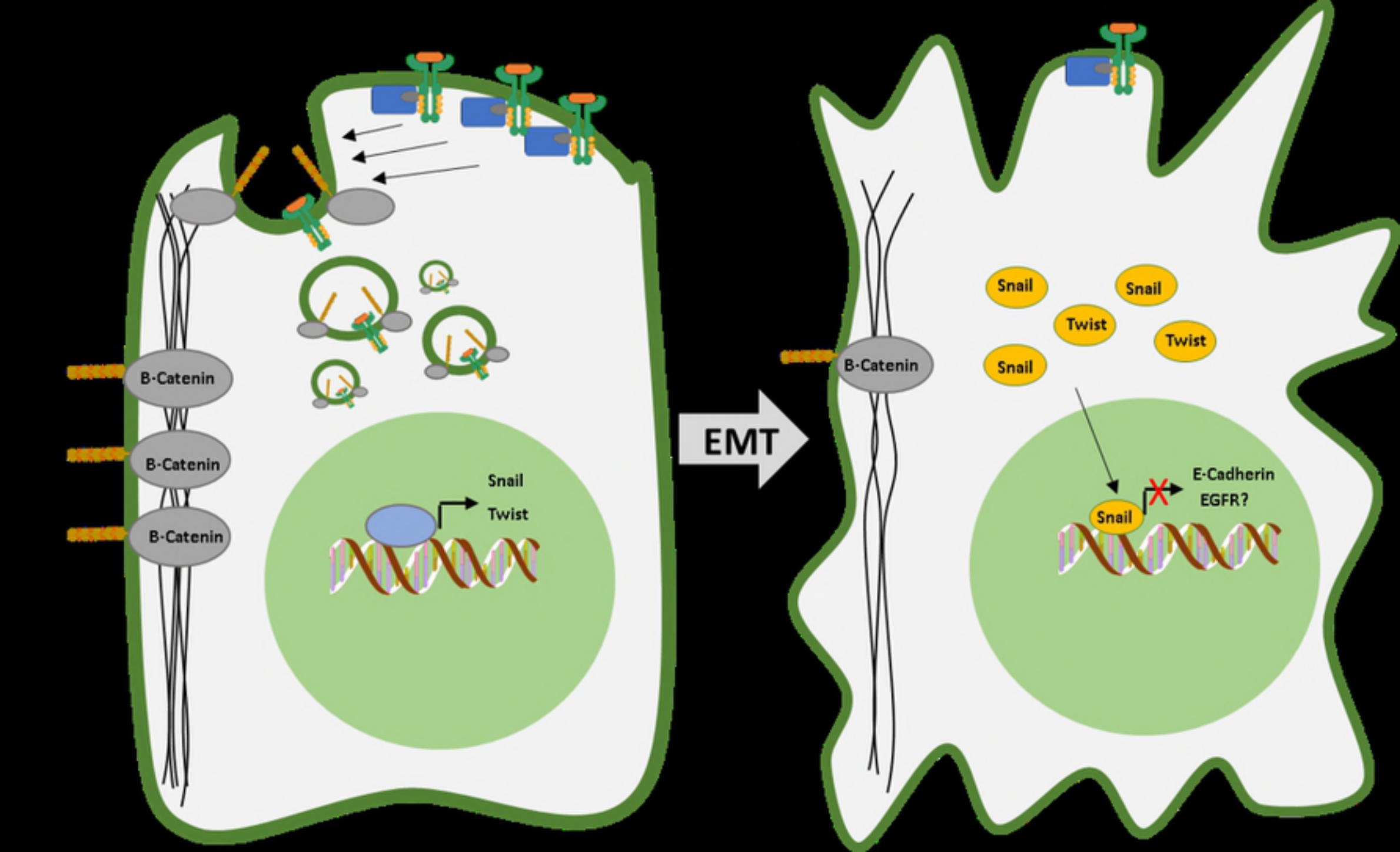
B-Catenin
B-Catenin
B-Catenin
Snail
Twist
EMT
B-Catenin
Snail
Snail
Twist
Twist
Snail
Snail
E-Cadherin
EGFR?